Article

Ion Mobility-Derived Collision Cross Section As an Additional Measure for Lipid Fingerprinting and Identification

Giuseppe Paglia,[†,‡] Peggi Angel,[§] Jonathan P. Williams,[‖] Keith Richardson,[‖] Hernando J. Olivos,[‖] J. Will Thompson,[⊥] Lochana Menikarachchi,[#] Steven Lai,[‖] Callee Walsh,[§] Arthur Moseley,[⊥] Robert S. Plumb,[‖,▽] David F. Grant,[#] Bernhard O. Palsson,[▽] James Langridge,[‖] Scott Geromanos,[‖] and Giuseppe Astarita*[‖,○]

[†]Istituto Zooprofilattico Sperimentale della Puglia e Della Basilicata, Foggia, Italy

[‡]Center for Systems Biology, University of Iceland, Reykjavik, Iceland

[§]Protea Biosciences Group, Inc., Morgantown, West Virginia 26505, United States

[‖]Waters Corporation, Milford, Massachusetts 01757, United States

[⊥]Duke Proteomics Core Facility, Durham, North Carolina 27708, United States

[#]Department of Pharmaceutical Sciences, University of Connecticut, Storrs, Connecticut 06268, United States

[▽]Computational and Systems Medicine, Department of Surgery and Cancer, Faculty of Medicine, Imperial College London, London, United Kingdom

[○]Department of Biochemistry and Molecular & Cellular Biology, Georgetown University, Washington, DC 20057, United States

S *Supporting Information*

ABSTRACT: Despite recent advances in analytical and computational chemistry, lipid identification remains a significant challenge in lipidomics. Ion-mobility spectrometry provides an accurate measure of the molecules' rotationally averaged collision cross-section (CCS) in the gas phase and is thus related to ionic shape. Here, we investigate the use of CCS as a highly specific molecular descriptor for identifying lipids in biological samples. Using traveling wave ion mobility mass spectrometry (MS), we measured the CCS values of over 200 lipids within multiple chemical classes. CCS values derived from ion mobility were not affected by instrument settings or chromatographic conditions, and they were highly reproducible on instruments located in independent laboratories (interlaboratory RSD < 3% for 98% of molecules). CCS values were used as additional molecular descriptors to identify brain lipids using a variety of traditional lipidomic approaches. The addition of CCS improved the reproducibility of analysis in a liquid chromatography-MS workflow and maximized the separation of isobaric species and the signal-to-noise ratio in direct-MS analyses (e.g., "shotgun" lipidomics and MS imaging). These results indicate that adding CCS to databases and lipidomics workflows increases the specificity and selectivity of analysis, thus improving the confidence in lipid identification compared to traditional analytical approaches. The CCS/accurate-mass database described here is made publicly available.
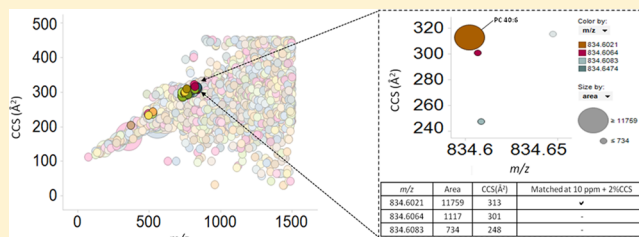
Fueled by novel analytical technologies and a resurgent interest in lipid biochemistry, lipidomics has become a widely accepted analytical approach for biomarker discovery and translational medicine.[1−4] Alterations in lipid metabolism have been associated with various human diseases, including metabolic syndrome and Alzheimer's disease.[2,5,6] Recently, lipidomic studies based on mass spectrometric analysis have identified, characterized, and quantified almost 600 lipid molecular species in human plasma.[7] It is predicted, however, that thousands of currently unknown lipids exist in biological samples.[2,7,8] To partially address this problem, MS and MS/MS lipid databases have been developed using both reference standards and *in silico* methods.[8−13] Yet because of the variety and complexity inherent in lipid structures, MS-based lipid

identification remains the most challenging step in a lipidomic workflow.

Historically, chromatographic separation has been used to maximize lipid separation prior to MS detection. More recently, a gas-phase separation tool such as traveling-wave ion mobility (TWIM) has been used in combination with MS. The combined approach facilitates lipid analysis[14] by increasing peak capacity,[15,16] improving structural elucidation,[17−19] and separating isomeric species.[15,20−23] In TWIM-MS, an ion-mobility separation stage consisting of a stacked-ring ion guide

with RF confinement is filled with an inert gas such as nitrogen. Ions travel through the gas toward the MS detector propelled in an axial direction by a traveling-wave, DC voltage.[24] Ions are thus separated in the gas phase according to their mobility through the gas, which is related to the ions' charge, shape, and size.

The time required for an ion to transverse the ion-mobility separation cell is called drift time. From the drift time values, it is possible to derive the rotationally averaged collision cross section (CCS), which represents the effective area for the interaction between an individual ion and the neutral gas through which it is traveling.[25−28] Thus, in addition to accurate mass data, ion mobility-derived CCS provides an additional physicochemical measurement that can be used for lipid annotation and identification.

In this multilaboratory study, we investigated the use of ion mobility-derived CCS as an additional molecular descriptor for lipid identification using a variety of traditional lipidomics approaches. In addition, we generated a publicly available database, containing CCS and accurate-mass values, to support lipid identification.

■ MATERIAL AND METHODS

All chemicals were purchased from Sigma-Aldrich (Seelze, Germany) and were of analytical grade, or higher, purity. Fatty acids were purchased from Cayman Chem (Ann Arbor, Michigan USA) and Nu-Chek (Elysian, Minnesota USA). The remaining lipid standards were all purchased from Avanti Polar Lipids (Alabaster, Alabama USA), including 1-stearoyl-2-arachidonoyl-*sn*-glycero-3-phosphocholine, 1,2-dioleoyl-*sn*-glycero-3-phosphocholine, 1-stearoyl-2-docosahexaenoyl-*sn*-glycero-3-phosphoethanolamine, ceramides, cholesterol, natural lipid classes purified from animal tissues, and total lipid extracts from porcine brain, *E. coli*, and yeast (See Table S1 in the Supporting Information for additional information). Frozen human brain samples (frontal cortex; age = 75.5 ± 5.0 years; average, post-mortem interval = 3.2 ± 0.4 h; $n = 6 \pm$ SD) were obtained from the Banner Sun Health Research Institute (Sun City, Arizona USA). All subjects or their caregivers, where applicable, provided written, informed consent for the clinical examination as well as for brain donation at the Banner Sun Health Research Institute Brain and Body Donation Program. The protocols and informed consent have been approved by the Banner Health Institutional Review Board.

Lipid Extractions. Frozen brain samples were rapidly weighed and homogenized in ice-cold methanol (1 v). Lipids were extracted by adding chloroform (2 v) and water (1 v) and centrifuged at 10 000g for 10 min at 4 °C. The bottom phases were dried under nitrogen, reconstituted in isopropanol/acetonitrile/water (4:3:1, v/v/v; 0.1 mL), and subjected to further analysis.

CCS Measurements. Traveling wave ion mobility mass spectrometers (Synapt G2 HDMS, Waters, Corporation, Manchester, UK), located in different laboratories, were used to derive CCS values for various lipid classes. A mass range of m/z 50−1500, with the mass spectrometer operating in both positive and negative electrospray ionization, was used. A summary of the MS settings appears in Table S2 (Supporting Information). Direct injection at 5 μL/min was used. CCS values, obtained in nitrogen, were experimentally determined using previously published CCS values for singly charged polyalanine oligomers as the TWIM calibrant species in both ESI$^+$ and ESI$^-$ mode[26,27] (Table S3 in the Supporting

Information). Poly-DL-alanine was prepared in 50:50 (v/v) water/acetonitrile at a concentration of 10 mg/L. Calibration was performed using singly charged oligomers from $n = 3$ to $n = 14$. The calibration encompassed a mass range extending from 231 to 1012 Da and a CCS range extending from 151 Å^2 to 306 Å^2, in ESI$^+$, and from 150 Å^2 to 308 Å^2, in ESI$^-$ (Table S3 in the Supporting Information).[26] CCS values were derived according to previously reported procedures.[26,28] The ion-mobility resolution was ~40 $\Omega/\Delta\Omega$(fwhm). The ion-mobility peak, or arrival-time distribution (ATD), may represent a combination of structurally similar isomers that remain unresolved. The CCS values reported were determined at the apex of the ATD.[29]

UHPLC-TWIM-MS Lipidomic Analysis. Lipidomic analyses of brain samples were performed with a microfluidics ionKey/MS system composed of an ACQUITY UPLC M-Class, the ionKey source, and an iKey CSH C18 130 Å, 1.7 μm particle size, 150 μm × 100 mm column (Waters Corporation, Milford, Massachusetts, USA) coupled to a Synapt G2-Si (Waters Corporation, Manchester, UK). Analyses were conducted in both positive and negative electrospray mode. The capillary voltage was 2.8 kV and the source temperature 110 °C. Injections were 0.5 μL using partial-loop mode, with a column temperature of 55 °C and flow rate of 3 μL/min. Mobile phase A consisted of acetonitrile/water (60:40) with 10 mM ammonium formate +0.1% formic acid. Mobile phase B consisted of isopropanol/acetonitrile (90:10) with 10 mM ammonium formate +0.1% formic acid. The gradient was programmed as follows: 0.0−2.0 min from 40% B to 43% B, 2.0−2.1 min to 50% B, 2.1−12.0 min to 99% B, 12.0−12.1 min to 40% B, and 12.1−14.0 min at 40% B.

TWIM-MS Tissue Imaging. Frozen, human, brain samples were serially sectioned in a cryostat, to allow alternate microscopic and MS-imaging analyses. Sections were placed on standard microscope slides and kept frozen at −15 °C throughout the analysis using the Peltier cooled stage of the Laser Ablation Electrospray Ionization (LAESI) DP-1000. Sections were analyzed using the LAESI DP-1000 Direct Ionization System (Protea Bioscience, Morgantown, West Virginia, USA) coupled with a Synapt G2-S mass spectrometer (Waters Corporation, Manchester, UK). The electrospray solution for LAESI was methanol/water (50:50, v/v) with 0.1% acetic acid. LAESI-TWIM-MS parameters consisted of 10 laser pulses per pixel at 5 Hz and 800 uJ of laser energy. Data were collected in both negative- and positive-ion mode using a mass range of m/z 50 to 1500 for MS scans as well as for ion-mobility-MS scans. Identifications were made according to accurate-mass and CCS values. Selected drift-time regions were extracted using Driftscope (Waters Corporation, Manchester, U.K.). Ion distribution maps were created for mass values of interest using ProteaPlot v2.0.3.8 (Protea Bioscience, Morgantown, West Virginia, USA).

Data Processing and Analysis. Data processing, quantitative analysis, and database searches were conducted using Progenesis QI Informatics (Nonlinear Dynamics, Newcastle, U.K.). Each UHPLC-TWIM-MS run was imported as an ion-intensity map including m/z and retention time. The software automatically converted drift time data to CCS values using the polyalanine calibration. Lipids were identified by searching publicly available databases (i.e., Human Metabolome Database (HMDB),[11] METLIN,[12] and LipidsMaps[8]) and in-house databases containing masses, retention times, fragment information, and ion mobility-derived CCS values.
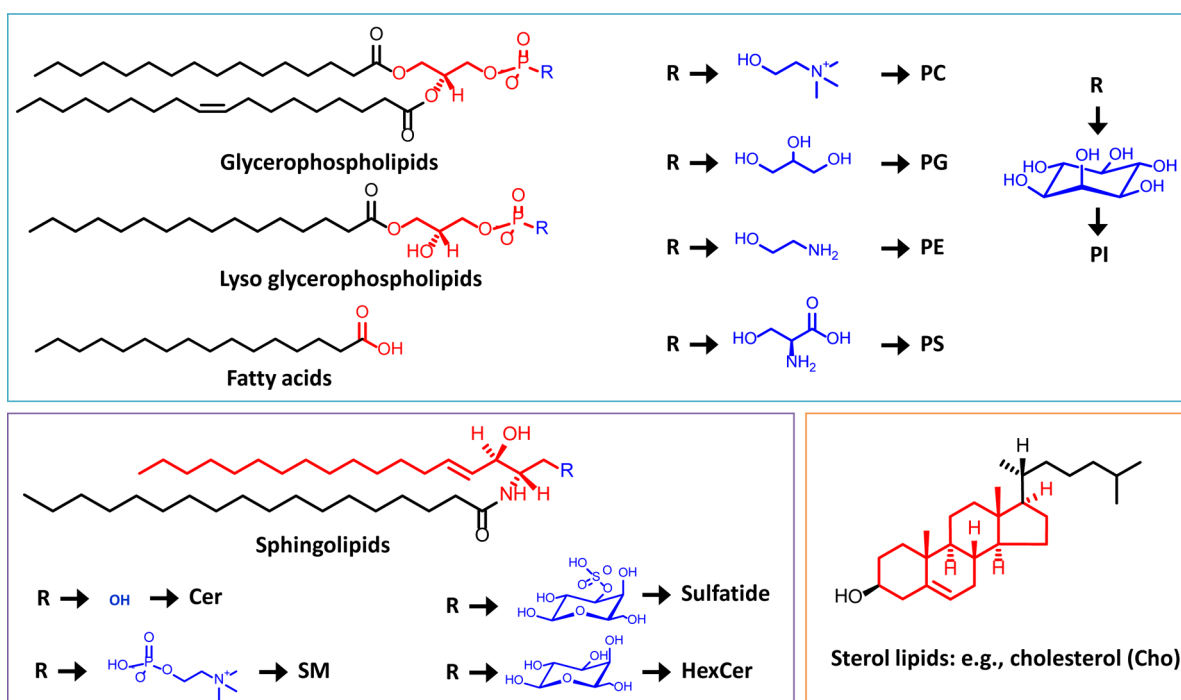
Figure 1. Lipid classes analyzed in this study. Categorization of lipids based upon their chemical structures. Highlighted in red are the core-structures from which the various lipid classes take their name. Highlighted in blue are the functional groups from which the various lipid subclasses take their name. Abbreviations: PC, phosphatidylcholine; PE, phosphatidylethanolamine; PS, phosphatidylserine; PG, phosphatidylglycerol; PI, phosphatidylinositol; Cer, ceramide; SM, sphingomyelin; HexCer, hexosyl ceramide; Cho, cholesterol.
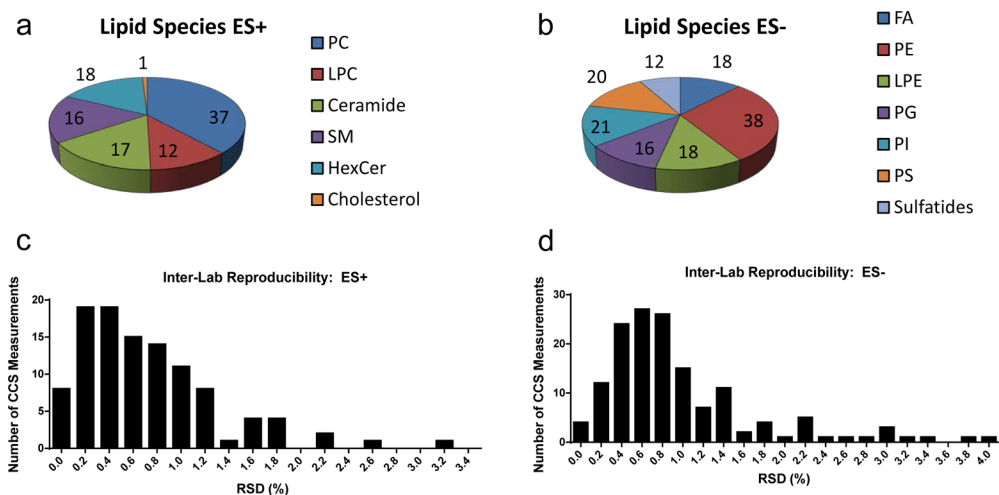

Figure 2. A CCS database for lipids. A total of 244 lipids were included in the CCS database. CCS values were obtained for different lipid classes and subclasses in both positive ESI⁺ (a) and negative ESI⁻ ionization (b). Frequency distribution plot of Relative Standard Deviations (RSD) obtained for the CCS measurements of the lipid species across different laboratories in both positive (c) and negative (d) ionization mode.

■ RESULTS AND DISCUSSION

We recently reported the first CCS database for polar metabolites, showing its applicability and utility in supporting metabolomics experiments.[28] In the present study, we extended our previous investigation by implementing ion mobility-derived CCS in routine lipidomics workflows. In a multi-laboratory effort, we calculated CCS values of an array of common lipid classes (Figure 1), generating a searchable database containing CCS and accurate-mass values (Tables S4 and S5 in Supporting Information). This database was then used as an aid in identifying lipids from brain samples.

Ion Mobility-Derived CCS Values for Lipids. To implement the use of ion mobility in routine MS-based lipidomics workflows, we measured the CCS of the most common lipid classes in independent laboratories (Figure 2a,b). We obtained CCS values for 244 lipids representing 13 lipid classes (101 values in positive ion mode and 143 values in negative ion mode; Tables S4 and S5 in the Supporting Information) with an inter-laboratory RSD lower than 3% for 98% of the measurements (Figure 2c,d). These results highlight the fact that, as previously reported for polar metabolites,[28] CCS values of lipids are highly reproducible, independently of the particular experimental conditions employed (Table S2 in
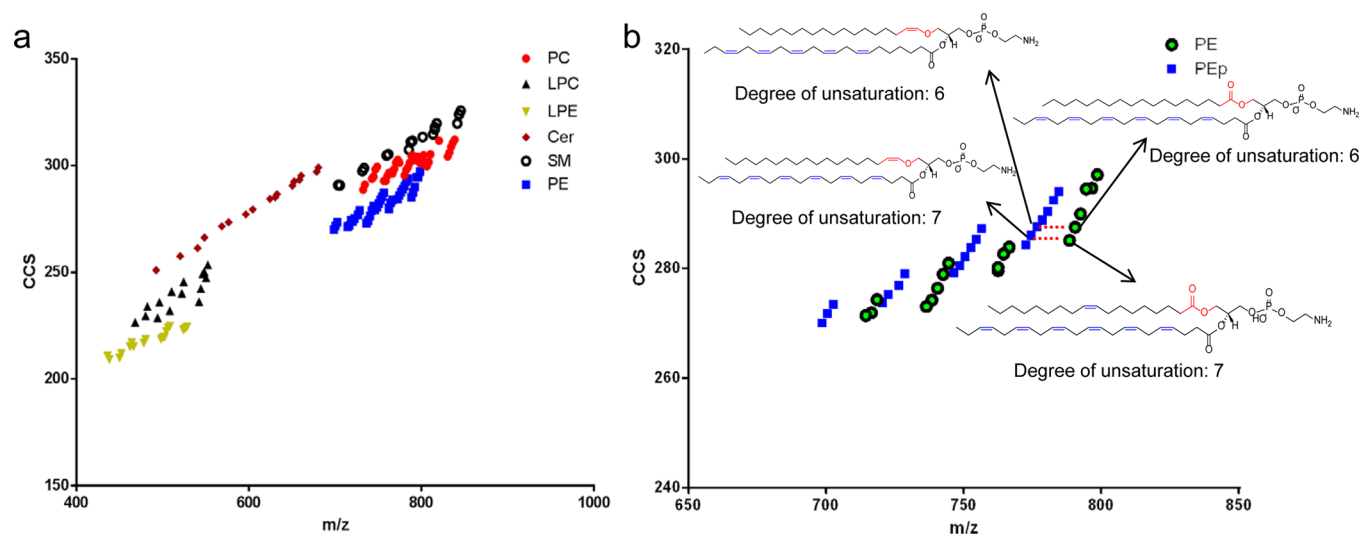
Figure 3. Mass versus CCS correlation curves for various lipid classes. (a) Lipids classes were grouped on the basis of their *m/z* and CCS values. (b) Representative separation of the lipid subclasses phosphatidylethanolamine (PE, green dots) and plasmalogen PE (PEp, blue squares), which were tentatively identified.
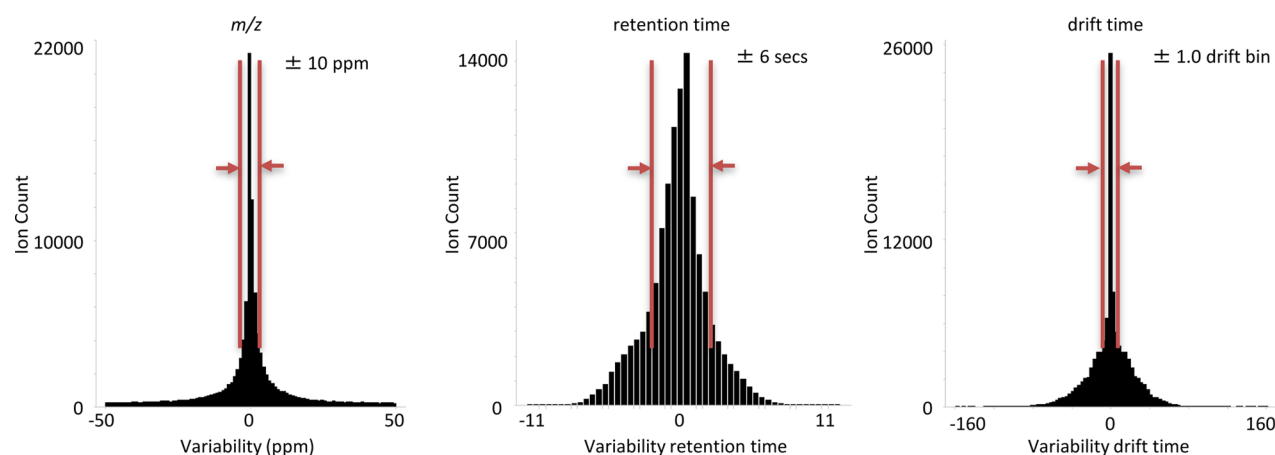

Figure 4. Intra-lab reproducibility and specificity of analysis by separation method. The half height widths for each of the three measured distributions (*m/z*, retention time and drift time) for the human brain lipidome across six samples, showing higher reproducibility of drift time measurements compared to retention time values.

the Supporting Information). This reproducibility is the result of the stability of the ion mobility technology as well as the use of calibrants that correct for variation in the instruments' drift times.

To our knowledge, this is the first report providing CCS values for lipid anions. The CCS values for the lipid cations agree with those previously reported in the literature, deriving both from standard tissue extracts measured with drift tubes[29,30] or standard lipids measured with TWIM-MS[17,18] (Table S6 in the Supporting Information). Such evidence indicates that power fit calibration of the TWIM-MS device provides accurate and reliable CCS values in good agreement with those obtained from drift tube studies.[31]

Ion mobility CCS measurements can, by inference, provide information about the shape of lipid molecules. Extending what has already been found in previous studies,[14,18,32,33] CCS of various lipid classes (e.g., phosphatidylcholines and sphingomyelins) and lipid subclasses (e.g., vinyl ether phosphatidylethanolamines and acyl phosphatidylethanolamines) fell into distinct trend lines on an *m/z*-versus-CCS chart, according to their chemical structures (Figure 3a and b). To confirm lipid

identities, we relied on HDMS[E] acquisition mode, in which precursor ions are fragmented in a collision cell after the TWIM separation as previously reported.[15,16,19,28] These results suggest that CCS values provide an additional coordinate of information for lipid identification and structure confirmation.

To test the accuracy and precision of the CCS measurements in different matrices, we compared the CCS values in our database with those derived from a range of lipid extracts including porcine brain, *E. coli* and yeast (Figure S1 in the Supporting Information). Our results show that CCS values for the same lipids are conserved between different extracts, indicating high reproducibility of CCS measurements in varying matrices. These results also demonstrate the wide applicability of our database across lipid extracts of various origins to support lipid identification (Figure S1 in the Supporting Information).

Lipid identification is a critical step for converting data into meaningful biological results.[8,11,12,34,35] In a typical MS-based lipidomic experiment, features of interest are usually searched against databases that list physicochemical properties descriptive of each lipid (e.g., accurate mass). A minimum of at least
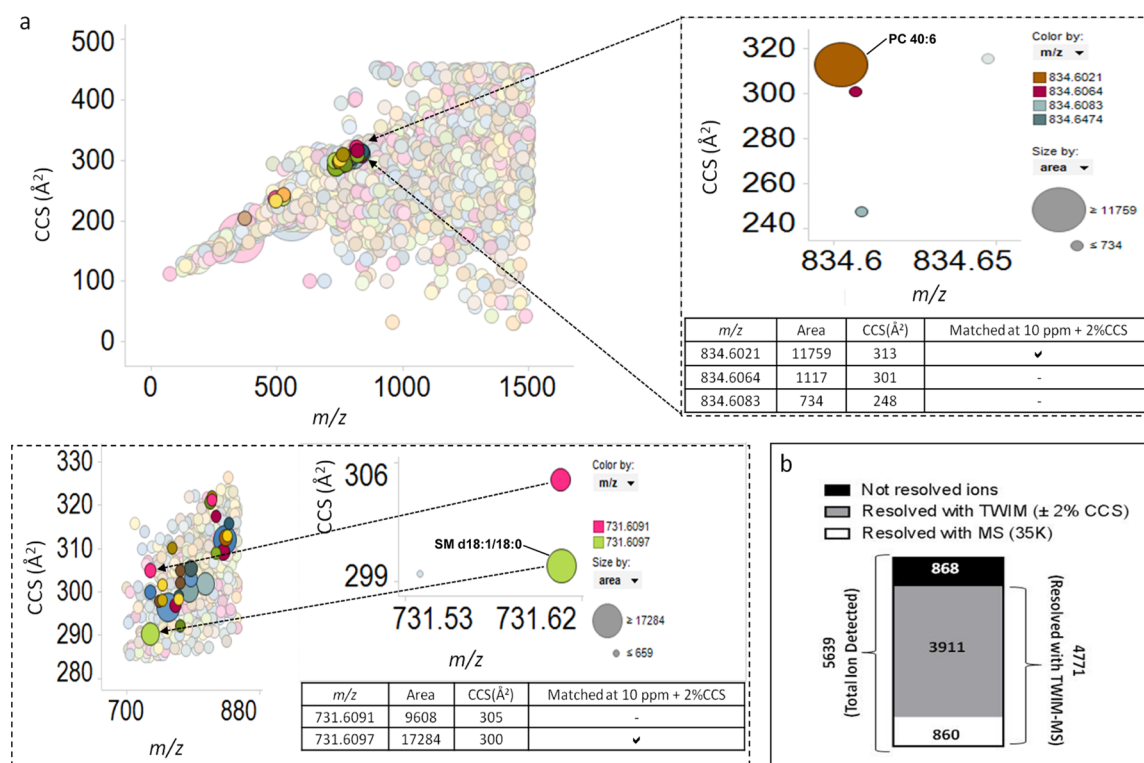
Figure 5. CCS in support of shotgun lipidomics. (a) Lipid extracts from porcine brain were directly infused in the TWIM-MS in positive ESI mode. Lipids were separated into two dimensions according to both CCS and *m/z*. The additional CCS coordinate allowed separation and identification of near isobaric lipids, including SM d18:1/18:0 at *m/z* 731.6097 and PC 40:6 at *m/z* 834.6021, increasing the specificity of analysis. (b) At 35 000 mass resolution, about 15% of the total 5639 ions were independently measured. The addition of CCS allowed independent measurment of about 85% of the total ions, increasing peak capacity.

two physicochemical measures are required for confident lipid identification.[36] In this context, a TWIM-MS experiment provides two measurements for lipids identification (i.e., accurate mass and CCS measurements) in a single acquisition. By annotating the accurate-mass and CCS values for each species, we created a unique database of common lipids available as a resource to the wider IM-MS community (Tables S4 and S5, in the Supporting Information).

A UHPLC-MS Lipidomic Workflow That Exploits CCS Information. To exploit the use of ion-mobility-derived CCS information in a typical lipidomic experiment, we analyzed human brain samples by microscale UHPLC/TWIM-MS using an integrated microfluidic device. The goal of this experiment was to improve the confidence in lipid identification from biological samples using CCS as an additional coordinate of information.

An in-depth analysis of the UHPLC/TWIM-MS data revealed that each brain sample contained more than 25 000 detectable ions. Each ion was associated with characteristic *m/z*, retention time, and CCS values. Ions consistently present in all samples were matched according to *m/z* < 10 ppm, retention time <6 s, and drift time <1 bin, resulting in 5151 detectable ions found in all six experiments. The mean intralaboratory analytical precision was RSD ~0.2% for CCS values, compared with RSD ~ 0.5% for retention-time values, which is in agreement with a previous report showing that CCS measurements are more stable and reliable than retention-time values (Figure 4).[28] Our results indicate that CCS, because of its stability and reproducibility, increases the degrees of freedom in matching ions between data sets, improving the accuracy and

precision of both qualitative and quantitative measurements for lipidomics analysis.

To identify the ions, we first performed isotope and adduct deconvolution. We then searched their accurate masses against publicly available databases, including LipidMaps,[8] HMDB,[11] and Metlin.[12] This process disclosed more than 1300 putative candidate identifications. Next, we cross-searched those potential identifications against our CCS lipid database, applying ΔCCS <3% as the difference between reference CCS values in our database and the experimental CCS values. The combination of CCS and accurate mass increased the confidence of identification for 137 lipids (red dots in Figure S2 in the Supporting Information). Such results indicate that applying CCS information can reduce the complexity of UHPLC-MS lipidomic results, facilitating rapid and reliable data interpretation.

Direct Analysis-MS Lipidomics Using CCS Information. Lipid databases containing CCS values may be of particular significance for interpreting direct-infusion MS—"shotgun" lipidomics—or desorption ionization-MS (e.g., MS imaging) lipidomic experiments. Such interpretations usually rely exclusively on one physicochemical measurement (i.e., accurate mass) for lipid fingerprinting and identification.[37−41] To test this hypothesis, we exploited CCS information in typical shotgun lipidomics and MS-imaging experiments.

CCS to Support Direct-Infusion, or Shotgun, Lipidomics. Commonly referred to as "shotgun" lipidomics, direct infusion of lipid extracts into a mass spectrometer without prior chromatographic separation provides an approach for high-throughput lipidomics.[42] Yet the approach suffers from a
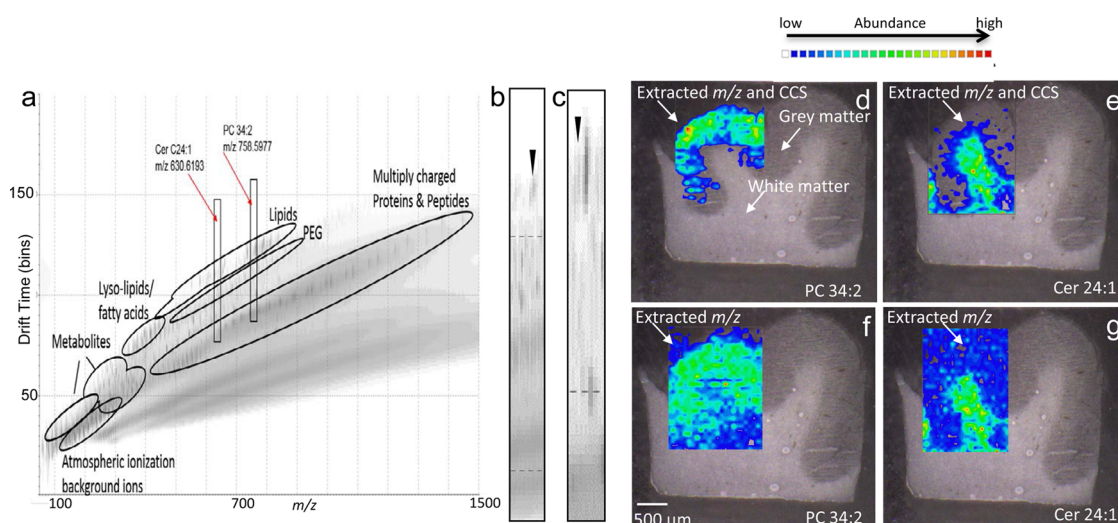
Figure 6. CCS in support of MS imaging. Identification and spatial localization of selected lipid species in human brain sections using LAESI-TWIM-MS. (a) Desorption ionization of human brain samples generated complex spectra composed of metabolites, lipids, and proteins that were separated in a bidimensional plot by both m/z and ion mobility. Red arrows denote two lipid species, Ceramide C24:1 (Cer C24:1) and PC 34:2, overlapping in the m/z dimension with near isobaric species but having different drift times. Close-up of drift regions for Cer C24:1 (b) and for PC 34:2 (c). (d) MS imaging of human brain showed a marked localization in the gray matter for the extracted ion at m/z 758.5977 (4.7 ppm) and CCS 294.1 Å^2 (ΔCCS< 1%) corresponding to PC 34:2 [M + H]$^+$; (e) MS imaging of human brain depicted a selected localization in the white matter for the extracted ion at m/z 630.6193 (−1.5 ppm) and CCS 282.5 Å^2 (ΔCCS< 1%) corresponding to Cer C24:1, [M-H$_2$O+H]$^+$; MS imaging of human brain generated using m/z values, without CCS selection, for PC 34:2 (f) and Cer C24:1 (g) showed low specificity and low signal-to-noise, which ultimately affected spatial resolution.

reduced ability to distinguish isobaric and isomeric species in crude lipid extracts.[14,29,43]

To evaluate the applicability of CCS information to a shotgun lipidomic analysis, we infused commercially available lipid extracts from porcine brain samples directly into the ESI-TWIM mass spectrometer, in positive ionization mode (5 μL/min per 1 min).[14,29,43] A 30 s slice of the infusion was processed with the detection algorithm Apex3D utilizing a fixed chromatographic peak width of 30 s.[44] Lipids were separated in two dimensions, according to CCS and m/z (Figure 5a). The additional dimension of ion-mobility separation increased the peak capacity of a traditional direct-infusion MS experiment more than 5-fold (Figure 5b), agreeing with previous reports.[32,45] Without CCS, at a mass resolution of 35 000 (fwhm), we were able to measure 860 independent ions, 15% of the 5639 total ions counted (Figure 5b). Thus, the addition of CCS allowed the resolution of 3911 additional ions (Figure 5b). The observed increase in peak capacity of analysis ultimately allows separation of isobaric species improving lipid fingerprinting and quantification in shotgun lipidomics applications.

We further examined the brain data set using our CCS lipid database to evaluate the use of mass accuracy alone versus combining CCS with mass accuracy for identification. A cutoff of 10 ppm and CCS ± 2% in our database search criteria allowed us to identify, with high confidence, 34 brain-lipid species, including SM d18:1/18:0 and PC 40:6 (Figure 5a; Tables S7 and S8 in the Supporting Information). Applying a cutoff of 10 ppm without any CCS filter, we found 21 mismatched lipid identifications (false positives), compared with the results obtained using 10 ppm and CCS as filters (Tables S7 and S8 in the Supporting Information). Furthermore, applying a cutoff of 5 ppm without CCS, we found nine mismatches and 13 missed matches (false negatives), compared with the results obtained using 10 ppm

and CCS as filters (Tables S7 and S8 in the Supporting Information). These results indicate that CCS allows for applying an additional set of tolerance criteria to shotgun lipidomics experiments, which might result in a reduced number of false-negative and false-positive identifications, ultimately leading to more confident compound identification.

CCS to Support MS Imaging. MS imaging provides the detailed spatial distribution of lipid species on biological tissues. Lipids are prominent features in MS imaging spectra of biological tissues under most desorption ionization sources, including matrix-assisted laser desorption ionization (MALDI)[16,46,47] and desorption electrospray ionization (DESI).[48,49] Two significant challenges in MS imaging experiments are (*i*) accurate lipid localization, which may be affected by the presence of confounding isobaric species,[41] and (*ii*) lipid identification, which relies, mostly, on accurate mass, because of the impractical nature of conducting a large number of MS/MS experiments on a single tissue section.[37,40,50]

To exploit the use of CCS information to improve MS-imaging applications, we analyzed human brain samples using LAESI coupled to a TWIM-MS instrument. Using CCS information allowed us to isolate lipids from metabolites, multiply charged proteins, and peptides, and from the background ions associated with atmospheric ionization (Figure 6a−c). Identities of 93 lipid species were confirmed by means of both accurate-mass and CCS measurements. Topographical maps representing the lipid ion distribution in subregions of the human brain were created for selected mass and CCS values present in gray matter (Figure 6d) and white matter (Figure 6e). The use of ion mobility allowed the spatial separation of isobaric lipid species with different CCS values, improving the quality of the signal-to-noise ratio (Figure 6f,g). Notably, only by using this approach was it possible to determine the selective spatial localization of PC 34:2 in the gray matter versus ceramide C24:1 in white matter. These

results indicate that CCS information may be a significant tool supporting lipid identification and localization in MS imaging studies.

CONCLUSIONS

In this study, we implemented the use of ion mobility-derived CCS measurements in lipidomics workflows to improve the specificity of data analysis and to facilitate lipid identification. We measured CCS values for over 200 common lipids in both positive- and negative-ion mode across independent laboratories. The measurements showed high reproducibility, and they were uninfluenced by instrument settings and chromatographic conditions. We annotated these CCS values in a unique lipid database, now available to everyone. When added to a liquid chromatography-MS-based lipidomics workflow, CCS data improved the reproducibility of analysis. When added to direct-MS lipidomics approaches (e.g., "shotgun" lipidomics and MS imaging), CCS measurements maximized the separation of isobaric species and increased the signal-to-noise ratio. Overall, our study demonstrates that the addition of CCS in databases and lipidomic workflows improves the accuracy and precision of analysis and thus the confidence in lipid assignment compared to traditional analytical approaches. We encourage further studies to extend and populate existing lipid databases with CCS values for lipid applications.

ASSOCIATED CONTENT

Ⓢ Supporting Information
Procedure for manually deriving CCS using a Synapt HDMS, Figures S1 and S2, and Tables S1−S8. This material is available free of charge via the Internet at http://pubs.acs.org.

AUTHOR INFORMATION

Corresponding Author
*E-mail: giuseppe_astarita@waters.com.
Notes
The authors declare no competing financial interest.

ACKNOWLEDGMENTS

REFERENCES

(1) Wenk, M. R. *Nat. Rev. Drug Discovery* **2005**, *4*, 594−610.
(2) Quehenberger, O.; Dennis, E. A. *N. Engl. J. Med.* **2011**, *365*, 1812−1823.
(3) Murphy, R. C.; Gaskell, S. J. *J. Biol. Chem.* **2011**, *286*, 25427−25433.
(4) Wenk, M. R. *Cell* **2010**, *143*, 888−895.
(5) Grimm, M. O.; Grimm, H. S.; Patzold, A. J.; Zinser, E. G.; Halonen, R.; Duering, M.; Tschape, J. A.; De Strooper, B.; Muller, U.; Shen, J.; Hartmann, T. *Nat. Cell Biol.* **2005**, *7*, 1118−1123.
(6) Mapstone, M.; Cheema, A. K.; Fiandaca, M. S.; Zhong, X.; Mhyre, T. R.; Macarthur, L. H.; Hall, W. J.; Fisher, S. G.; Peterson, D.

R.; Haley, J. M.; Nazar, M. D.; Rich, S. A.; Berlau, D. J.; Peltz, C. B.; Tan, M. T.; Kawas, C. H.; Federoff, H. J. *Nat. Med.* **2014**, in print.
(7) Quehenberger, O.; Armando, A. M.; Brown, A. H.; Milne, S. B.; Myers, D. S.; Merrill, A. H.; Bandyopadhyay, S.; Jones, K. N.; Kelly, S.; Shaner, R. L.; Sullards, C. M.; Wang, E.; Murphy, R. C.; Barkley, R. M.; Leiker, T. J.; Raetz, C. R.; Guan, Z.; Laird, G. M.; Six, D. A.; Russell, D. W.; McDonald, J. G.; Subramaniam, S.; Fahy, E.; Dennis, E. A. *J. Lipid Res.* **2010**, *51*, 3299−3305.
(8) Fahy, E.; Subramaniam, S.; Murphy, R. C.; Nishijima, M.; Raetz, C. R.; Shimizu, T.; Spener, F.; van Meer, G.; Wakelam, M. J.; Dennis, E. A. *J. Lipid Res.* **2009**, *50* (Suppl), S9−14.
(9) McDowell, G. S.; Blanchard, A. P.; Taylor, G. P.; Figeys, D.; Fai, S.; Bennett, S. A. *Biomed. Res. Int.* **2014**, *2014*, 818670.
(10) Kind, T.; Liu, K. H.; Lee do, Y.; DeFelice, B.; Meissen, J. K.; Fiehn, O. *Nat. Methods* **2013**, *10*, 755−758.
(11) Wishart, D. S.; Jewison, T.; Guo, A. C.; Wilson, M.; Knox, C.; Liu, Y.; Djoumbou, Y.; Mandal, R.; Aziat, F.; Dong, E.; Bouatra, S.; Sinelnikov, I.; Arndt, D.; Xia, J.; Liu, P.; Yallou, F.; Bjorndahl, T.; Perez-Pineiro, R.; Eisner, R.; Allen, F.; Neveu, V.; Greiner, R.; Scalbert, A. *Nucleic Acids Res.* **2013**, *41*, D801−807.
(12) Smith, C. A.; O'Maille, G.; Want, E. J.; Qin, C.; Trauger, S. A.; Brandon, T. R.; Custodio, D. E.; Abagyan, R.; Siuzdak, G. *Ther. Drug Monit.* **2005**, *27*, 747−751.
(13) Horai, H.; Arita, M.; Kanaya, S.; Nihei, Y.; Ikeda, T.; Suwa, K.; Ojima, Y.; Tanaka, K.; Tanaka, S.; Aoshima, K.; Oda, Y.; Kakazu, Y.; Kusano, M.; Tohge, T.; Matsuda, F.; Sawada, Y.; Hirai, M. Y.; Nakanishi, H.; Ikeda, K.; Akimoto, N.; Maoka, T.; Takahashi, H.; Ara, T.; Sakurai, N.; Suzuki, H.; Shibata, D.; Neumann, S.; Iida, T.; Funatsu, K.; Matsuura, F.; Soga, T.; Taguchi, R.; Saito, K.; Nishioka, T. *J. Mass Spectrom* **2010**, *45*, 703−714.
(14) Kliman, M.; May, J. C.; McLean, J. A. *Biochim. Biophys. Acta* **2011**, *1811*, 935−945.
(15) Shah, V.; Castro-Perez, J. M.; McLaren, D. G.; Herath, K. B.; Previs, S. F.; Roddy, T. P. *Rapid Commun. Mass Spectrom.* **2013**, *27*, 2195−2200.
(16) Hart, P. J.; Francese, S.; Claude, E.; Woodroofe, M. N.; Clench, M. R. *Anal. Bioanal. Chem.* **2011**, *401*, 115−125.
(17) Damen, C. W.; Isaac, G.; Langridge, J.; Hankemeier, T.; Vreeken, R. J. *J. Lipid Res.* **2014**, in print.
(18) Kim, H. I.; Kim, H.; Pang, E. S.; Ryu, E. K.; Beegle, L. W.; Loo, J. A.; Goddard, W. A.; Kanik, I. *Anal. Chem.* **2009**, *81*, 8289−8297.
(19) Castro-Perez, J.; Roddy, T. P.; Nibbering, N. M.; Shah, V.; McLaren, D. G.; Previs, S.; Attygalle, A. B.; Herath, K.; Chen, Z.; Wang, S. P.; Mitnaul, L.; Hubbard, B. K.; Vreeken, R. J.; Johns, D. G.; Hankemeier, T. *J. Am. Soc. Mass Spectrom.* **2011**, *22*, 1552−1567.
(20) Kaur-Atwal, G.; Reynolds, J. C.; Mussell, C.; Champarnaud, E.; Knapman, T. W.; Ashcroft, A. E.; O'Connor, G.; Christie, S. D.; Creaser, C. S. *Analyst* **2011**, *136*, 3911−3916.
(21) Ahonen, L.; Fasciotti, M.; Gennas, G. B.; Kotiaho, T.; Daroda, R. J.; Eberlin, M.; Kostiainen, R. *J. Chromatogr. A* **2013**, *1310*, 133−137.
(22) Dong, L.; Shion, H.; Davis, R. G.; Terry-Penak, B.; Castro-Perez, J.; van Breemen, R. B. *Anal. Chem.* **2010**, *82*, 9014−9021.
(23) Domalain, V.; Hubert-Roux, M.; Tognetti, V.; Joubert, L.; Lange, C.; Rouden, J. H.; Afonso, C. *Chem. Sci.* **2014**, *5*, 3234.
(24) Giles, K. *Int. J. Ion Mobility Spectrom.* **2013**, *16*, 69.
(25) Bush, M. F.; Hall, Z.; Giles, K.; Hoyes, J.; Robinson, C. V.; Ruotolo, B. T. *Anal. Chem.* **2010**, *82*, 9557−9565.
(26) Bush, M. F.; Campuzano, I. D.; Robinson, C. V. *Anal. Chem.* **2012**, *84*, 7124−7130.
(27) Williams, J. P.; Lough, J. A.; Campuzano, I.; Richardson, K.; Sadler, P. J. *Rapid Commun. Mass Spectrom.* **2009**, *23*, 3563−3569.
(28) Paglia, G.; Williams, J. P.; Menikarachchi, L.; Thompson, J. W.; Tyldesley-Worster, R.; Halldorsson, S.; Rolfsson, O.; Moseley, A.; Grant, D.; Langridge, J.; Palsson, B. O.; Astarita, G. *Anal. Chem.* **2014**, *86*, 3985−3993.
(29) Fenn, L. S.; Kliman, M.; Mahsut, A.; Zhao, S. R.; McLean, J. A. *Anal. Bioanal. Chem.* **2009**, *394*, 235−244.

(30) May, J. C.; Goodwin, C. R.; Lareau, N. M.; Leaptrot, K. L.; Morris, C. B.; Kurulugama, R. T.; Mordehai, A.; Klein, C.; Barry, W.; Darland, E.; Overney, G.; Imatani, K.; Stafford, G. C.; Fjeldsted, J. C.; McLean, J. A. *Anal. Chem.* **2014**, *86*, 2107−2116.

(31) Dear, G. J.; Munoz-Muriedas, J.; Beaumont, C.; Roberts, A.; Kirk, J.; Williams, J. P.; Campuzano, I. *Rapid Commun. Mass Spectrom.* **2010**, *24*, 3157−3162.

(32) Dwivedi, P.; Schultz, A. J.; Hill, H. H. *Int. J. Mass Spectrom.* **2010**, *298*, 78−90.

(33) Jackson, S. N.; Ugarov, M.; Post, J. D.; Egan, T.; Langlais, D.; Schultz, J. A.; Woods, A. S. *J. Am. Soc. Mass Spectrom.* **2008**, *19*, 1655−1662.

(34) Menikarachchi, L. C.; Cawley, S.; Hill, D. W.; Hall, L. M.; Hall, L.; Lai, S.; Wilder, J.; Grant, D. F. *Anal. Chem.* **2012**, *84*, 9388−9394.

(35) Zhu, Z. J.; Schultz, A. W.; Wang, J.; Johnson, C. H.; Yannone, S. M.; Patti, G. J.; Siuzdak, G. *Nat. Protoc.* **2013**, *8*, 451−460.

(36) Sumner, L. W.; Amberg, A.; Barrett, D.; Beale, M. H.; Beger, R.; Daykin, C. A.; Fan, T. W.; Fiehn, O.; Goodacre, R.; Griffin, J. L.; Hankemeier, T.; Hardy, N.; Harnly, J.; Higashi, R.; Kopka, J.; Lane, A. N.; Lindon, J. C.; Marriott, P.; Nicholls, A. W.; Reily, M. D.; Thaden, J. J.; Viant, M. R. *Metabolomics* **2007**, *3*, 211−221.

(37) Ridenour, W. B.; Kliman, M.; McLean, J. A.; Caprioli, R. M. *Anal. Chem.* **2010**, *82*, 1881−1889.

(38) O'Brien, P. J.; Lee, M.; Spilker, M. E.; Zhang, C. C.; Yan, Z.; Nichols, T. C.; Li, W.; Johnson, C. H.; Patti, G. J.; Siuzdak, G. *Cancer Metab.* **2013**, *1*, 4.

(39) Fasciotti, M.; Sanvido, G. B.; Santos, V. G.; Lalli, P. M.; McCullagh, M.; de Sa, G. F.; Daroda, R. J.; Peter, M. G.; Eberlin, M. N. *J. Mass Spectrom.* **2012**, *47*, 1643−1647.

(40) Woods, A. S.; Jackson, S. N. *Methods Mol. Biol.* **2010**, *656*, 99−111.

(41) Krakau, I.; Elkan, E. *Lakartidningen* **1988**, *85*, 3444.

(42) Han, X.; Gross, R. W. *Mass Spectrom. Rev.* **2005**, *24*, 367−412.

(43) Kaplan, K.; Dwivedi, P.; Davidson, S.; Yang, Q.; Tso, P.; Siems, W.; Hill, H. H., Jr. *Anal. Chem.* **2009**, *81*, 7944−7953.

(44) Geromanos, S. J.; Vissers, J. P.; Silva, J. C.; Dorschel, C. A.; Li, G. Z.; Gorenstein, M. V.; Bateman, R. H.; Langridge, J. I. *Proteomics* **2009**, *9*, 1683−1695.

(45) Dwivedi, P.; Puzon, G.; Tam, M.; Langlais, D.; Jackson, S.; Kaplan, K.; Siems, W. F.; Schultz, A. J.; Xun, L.; Woods, A.; Hill, H. H., Jr. *J. Mass Spectrom.* **2010**, *45*, 1383−1393.

(46) Fang, L.; Harkewicz, R.; Hartvigsen, K.; Wiesner, P.; Choi, S. H.; Almazan, F.; Pattison, J.; Deer, E.; Sayaphupha, T.; Dennis, E. A.; Witztum, J. L.; Tsimikas, S.; Miller, Y. I. *J. Biol. Chem.* **2010**, *285*, 32343−32351.

(47) Kettling, H.; Vens-Cappell, S.; Soltwisch, J.; Pirkl, A.; Haier, J.; Muthing, J.; Dreisewerd, K. *Anal. Chem.* **2014**, *86*, 7798−7805.

(48) Wiseman, J. M.; Ifa, D. R.; Song, Q.; Cooks, R. G. *Angew. Chem., Int. Ed.* **2006**, *45*, 7188−7192.

(49) Eberlin, L. S.; Norton, I.; Orringer, D.; Dunn, I. F.; Liu, X.; Ide, J. L.; Jarmusch, A. K.; Ligon, K. L.; Jolesz, F. A.; Golby, A. J.; Santagata, S.; Agar, N. Y.; Cooks, R. G. *Proc. Natl. Acad. Sci. U. S. A.* **2013**, *110*, 1611−1616.

(50) Garrett, T. J.; Yost, R. A. *Methods Mol. Biol.* **2010**, *656*, 209−230.